

Microstructure of aluminum twin-roll casting based on Cellular Automation

LIU Xiao-bo(刘晓波)¹, XU Qing-yan(许庆彦)², JING Tao(荆涛)², LIU Bai-cheng(柳百成)²

1. College of Mechanical and Electronic Engineering, Nanchang University, Nanchang 330031, China;
2. Department of Mechanical Engineering, Tsinghua University, Beijing 100084, China

Received 21 September 2007; accepted 23 April 2008

Abstract: Nucleation and growth model based on Cellular Automation(CA) incorporated with macro heat transfer calculation was presented to simulate the microstructure of aluminum twin-roll casting. The dynamics model of dendrite tip (KGT model) was amended in view of characteristics of aluminum twin-roll casting. Through the numerical simulation on solidification structure under different casting speeds, it can be seen that when the casting speed is 1.3 m/min, that is, under conditions of conventional roll casting, coarse columnar grains dominate the solidification structure, and equiaxed grains exist in the center of aluminum strip. When the casting speed continuously increases to 8 m/min, that is, under the conditions of thin-gauge high-speed casting, columnar grains in solidification structure all convert into equiaxed grains. Experimental and numerical results agree well.

Key words: twin-roll casting; aluminum microstructure; Cellular Automation(CA)

1 Introduction

Aluminum twin-roll casting is a new process, which turns liquid aluminum into strip directly. It puts the casting and hot rolling process of traditional aluminum strip into integration, on one hand, to complete continuous cooling and solidification, on the other hand, to produce plastic deformation. It has been widely used for its outstanding advantages, such as simple process, low energy consumption, short production cycle, low cost and low investment.

In the process of aluminum twin-roll casting, the microstructures of materials depend on the casting process parameters, and microstructure has a great impact on its properties. Therefore, to find out the disciplines of microstructure formation in roll casting is an economical and feasible way to optimize the parameters of casting process and to get high quality strip by the calculation and prediction of casting process.

In the recent ten years, many kinds of methods about solidification structure simulation have been

presented, which can be summed up in two main categories: deterministic simulation and stochastic simulation. Deterministic simulation, based on solidification dynamics, meets the physical background of grain growth, but some random phenomena in the process of grain growth cannot be considered, including the random distribution of grain nuclei, random orientation of the grain and the conversion from columnar grains to equiaxed grains and so on[1–3]. Phase-field model reflects the comprehensive role of the solute diffusion, order and thermodynamic driver. The shape, curvature and movement of solid/liquid interface of metal system can be described with the solution of field equations[4–9], and the metal solidification process can be realistically simulated. However, the computational domain is not large enough for actual roll casting. The two methods including Monte Carlo (called MC) method and Cellular Automation (called CA) are more representative among the stochastic methods. Probability theory is introduced to MC method to deal with the distribution of nucleation position and grain growth orientation at random. Images similar with the actual

metallography can be got by MC method, and the impact of different process parameters can be manifested[10–12]. However, MC simulation lacks physical infrastructure, and the simulation time-step has nothing to do with the actual solidification time. CA law was initially used to simulate the grain growth of recrystallization, and later it was introduced to simulate the formation of the grain in the solidification process by GANDIN and RAPPAZ [13–14]. Based on physical mechanism of the process of nucleation and kinetics of grain growth, the size and distribution of grain can be got, and the formation of columnar grains and the conversion from columnar grains to equiaxed grains can also be described by CA. In recent years, CA model has been used to study the phase transition in solidification process, and it has made a lot of progress[15–23]. Formation law of solidification microstructures in roll casting was studied in the present work by the established mathematical model of nucleation and grain growth based on CA.

2 Mathematical model

2.1 Nucleation model

Continuous nucleation model which was heterogeneous nucleation based on Gaussian distribution was used.

Assume that nucleation occurs at different positions, and these nucleation locations can be described by continuous rather than discrete distribution function, $dn/d(\Delta T)$. The density of grains $n(\Delta T)$ at a given undercooling ΔT is described by the integral of nucleation density distribution:

$$n(\Delta T) = \int_0^{\Delta T} \frac{dn}{d(\Delta T')} d(\Delta T') \quad (1)$$

$$\frac{dn}{d(\Delta T)} = \frac{n_{\max}}{\sqrt{2\pi}\Delta T_{\sigma}} \exp\left[-\frac{1}{2}\left(\frac{\Delta T' - \Delta T_N}{\Delta T_{\sigma}}\right)^2\right] \quad (2)$$

where ΔT_N is the mean nucleation undercooling, ΔT_{σ} is the standard curvature undercooling, and n_{\max} is the total density of grains.

2.2 Growth model

In KGT model, undercooling ΔT is composed of four parts:

$$\Delta T = \Delta T_C + \Delta T_R + \Delta T_T + \Delta T_K \quad (3)$$

The twin-roll casting process is a sub-rapid solidification with the nature of directional solidification, therefore, the dendrite growth velocity is not very high relatively to rapid solidification; the kinetic coefficient of alloys is great; and the kinetic undercooling of dendrite

tip can be neglected. As the solidification undergoes in the quasi-equilibrium condition, it can be deemed that the balanced distribution coefficient remains unchanged. Therefore, KGT model can be amended. The amended KGT model can be seen from the following equations:

$$\Delta T = \Delta T_C + \Delta T_R \quad (4)$$

$$R = 2\pi[\Gamma/(mG_{\epsilon}\zeta_c - G)]^{1/2} \quad (5)$$

$$\Omega = Iv(Pe) \quad (6)$$

$$v = 2DP_e/R \quad (7)$$

$$\Delta T_C = -(c_1^* - c_0)m_1 \quad (8)$$

$$\Delta T_T = -\gamma kf(\theta_i) \quad (9)$$

$$f(\theta_i) = \prod_{i=x,y,z} (1 + \gamma_i \cos(\lambda_i \theta_i)) \quad (10)$$

$$\theta_i = \arccos \frac{|P_1^* P_s^*|}{i_1 - i_s} \quad (11)$$

where ΔT is the undercooling, ΔT_C is the ingredient undercooling, ΔT_R is the curvature undercooling, ΔT_T is the thermal undercooling, ΔT_K is the kinetics undercooling, R is the growing radius of dendrite tip, Ω is the dendrite growth saturation, c_0 is the initial concentration of the alloy, c_1 is the solute concentration at the liquid interface, k is the solute partition coefficient, m is the slope of liquidus, Γ is the Gibbs-Thomson coefficient, G_{ϵ} is the solute concentration gradient in the forefront liquid of dendrite, G is the temperature gradient, Pe is the Peclet number of solute, $Iv(Pe)$ is the Ivantsov function of Peclet number, ζ_c is the function of Peclet number, v is the growth velocity of dendrite tip, D is the diffusion coefficient of the liquid phase, and θ_i is the angle between the largest grain growth direction and x -axis.

3 Numerical simulation

3.1 Mesh division

During the computing, larger mesh was used to simulate the temperature field, and the cell meshes with smaller size were used for simulation of micro nucleation and growth, then the micro cell temperature can be got by interpolation of macro cell temperature in space and time. Obviously, the temperature is influenced by its neighboring macro-cells, and it is in reverse ratio to the distance between the neighboring macro-cell and point a:

$$T_a = \sum_{i=1}^4 l_i^{-1} T_i / \sum_{i=1}^4 l_i^{-1} \quad (12)$$

where T_a is the temperature of the micro cell a, T_i is the temperature of the neighboring macro cell, and l_i is the distance from point a to the macro-cell.

The size of macro-cell is 10 mm × 10 mm, which is further divided into 100 × 100 micro cells.

3.2 Calculation of nucleation and growth

The nucleation density at a given time is described by the integral of $dn/d(\Delta T)$ in the interval (0, ΔT). When the cell temperature is lower than the liquidus, in a time step δT , the temperature decreases by δt , and the undercooling increases by $\delta(\Delta T)$ ($\delta(\Delta T) > 0$). The density of new grains is given by

$$\delta n_v = n_v[\Delta T + \delta(\Delta T)] - n_v(\Delta T) = \int_{\Delta T}^{\Delta T + \delta(\Delta T)} \frac{dn_v}{d(\Delta T')} d(\Delta T') \quad (13)$$

where the subscript symbol 'v' refers to the particle distribution of internal melt (as opposed to the wall). The number of new grains in this time-step δN_v is given by the multiplication of the grain density increase δn_v with the total volume of the melt V . These new grains are randomly distributed in the whole CA unit, and the probability is

$$p_v = \frac{\delta N_v}{N_{CV}} = \delta n_v V_{CA} \quad (14)$$

Each CA unit was given one random number n ($0 \leq n < 1$) in every time-step δt . If a unit is still liquid whose state index remains 0, when $n < p_v$, the solid-liquid phase transition occurred, and its state index would be given a positive integer to describe the different grain orientation. When the CA unit nucleated, it would grow with a certain law. In numerical calculation, the approaches are as follows.

In the two-dimensional plane, to divide the calculated zone into regional grids which are usually square or hexagon, the most adjacent modules of each unit are marked. A is a nucleation site in mesh grids which is nucleated at a certain time t_N . θ is the angle between the largest grain growth direction and x-axis, which is chosen randomly as $-45^\circ < \theta < 45^\circ$. At time t , the radius of grain $L(t)$ is the integral of growth velocity of dendrite tip along the whole growing time:

$$L(t) = \int_{t_N}^t v[\Delta T(t')] dt' \quad (15)$$

$v[\Delta T]$ can be calculated by KGT model. At the time t_B , the grain A grows and touches the four neighboring cells B1, B2, B3 and B4. At this time, the semi-diagonal of grain $L(t_B)$ is equal to $l_\theta = l(\cos\theta + |\sin\theta|)$, where l is the distance between every two CA mesh grids. CA model prescribes that B1, B2, B3 and B4 are considered to

become solid and assigned a crystallographic index as the same as A. The grain continues to grow and capture the neighboring liquid sites and form the final grain shape. B1, B2, B3 and B4 continues to grow and capture the eight sites of neighboring C at the next time, etc. The grain increases with the growth velocity of dendrite tip.

Some parameters used in the calculation are listed in Table 1.

Table 1 Partial thermophysical properties used in simulation

Thermal conductivity, $\lambda/(W \cdot m^{-1} \cdot ^\circ C^{-1})$		Specific heat, $C_v/(J \cdot m^{-3} \cdot ^\circ C^{-1})$	Latent heat, $L_v/(J \cdot m^{-3})$
241		296×10^6	9.5×10^8
Liquidus, $T_L/^\circ C$	Solidus, $T_S/^\circ C$	Partition coefficient, k	Slope of liquidus, $m/(^\circ C^{-1})$
659	615	0.117	-6

4 Results and discussion

The aluminum microstructure under different casting speeds was simulated and compared with the experimental results in the present work.

In order to observe the real solidification microstructures, after the roll casting experiment, that is, at casting machine downtime, feeding mouth should be distracted backwards rapidly from the roll by the transmission, and the wedge-shaped aluminum strip in the roll aperture should be taken out from the casting mouth side. Sampling positions locate in the casting zone, where the strip almost has no deformation. Samples are directly got from the formed aluminum strip along the rolling and horizontal direction, then processed into 15 mm-long specimen.

Metallographic samples with different casting process parameters were made through rough grinding, intensive grinding, mechanical polishing, electrochemical polishing and film anode technology. The microstructure of prepared metallographic samples was observed by NEOPHOT-21 metallographic microscope.

Solidification structures under the conditions of conventional roll casting and thin-gauge high-speed casting were adopted.

Simulated and experimental results of roll casting solidification microstructure at the casting speed of 1.3 m/min are shown in Fig.1. It can be seen from Fig.1(a) that when the casting speed is 1.3 m/min, the thickness of the strip is 6 mm. Under conditions of conventional roll casting, coarse columnar grains dominate the solidification microstructure, and equiaxed grains exist in the center of aluminum strip. This is because when the casting speed is small, the formed nucleus is "free" to the liquid zone from the roller surface, even form solidified shell, then the solidified grains grow ahead of the liquid

zone along the inverse direction of heat flow. At this time, because of the large undercooling of liquid/solid

state-interface, and the length of condensation district and nuclear-shaped area increases. At the same time, the

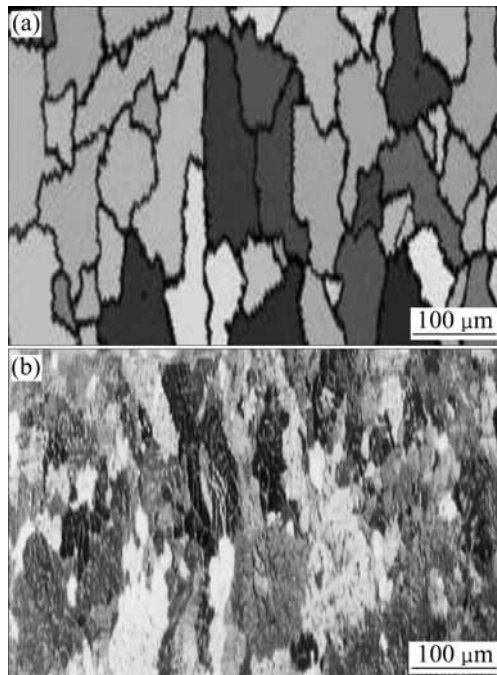


Fig.1 Simulated and experimental results of roll casting solidification structures at casting speed of 1.3 m/min: (a) Simulated results of roll casting structure; (b) Experimental results of roll casting structure

interface and the small temperature gradient, liquid/solid interface is stable, grains grow as columnar grains, and the curvature of columnar grains is as small as that of the non-planar interface. However, when few grain nuclei free from the roll surface or some non-spontaneous nucleation formed from foreign impurities exist in aluminum melt, liquid/solid interface will be localized unstable. These grains grow as a free grain growth, continue to impede the growth of columnar grains, and finally form equiaxed grains. Fig.1(b) shows a metallographic image of aluminum strip solidification microstructure at the casting speed of 1.3 m/min. This indicates that experimental and simulated results agree well.

Simulated and experimental results of roll casting solidification structures at the casting speed of 8 m/min are shown in Fig.2. It can be seen from Fig.2(a) that when the casting speed is 8 m/min, the thickness of the strip is 3 mm, and equiaxed grains dominate the entire thickness of aluminum strip. This is due to the fact that the further increase in casting speed makes the impingement flows of aluminum melt near roller surface enhance, which leads to the temperature fluctuations of the forefront liquid/solid interface and the instability of interface. Liquid/solid interface no longer maintains

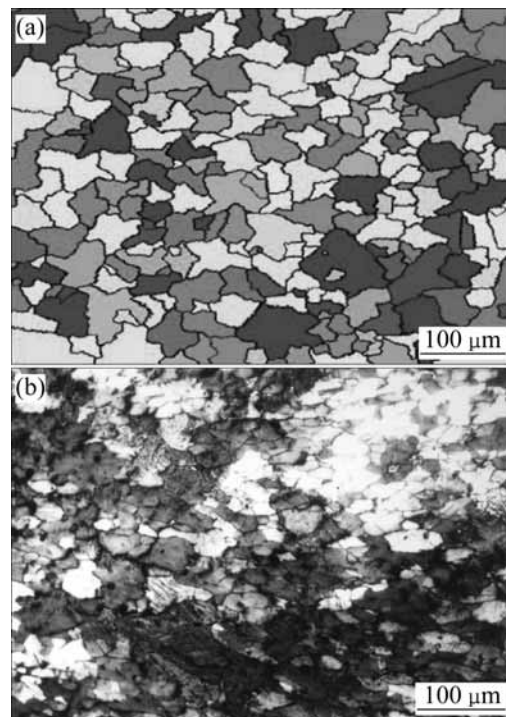


Fig.2 Simulated and experimental results of roll casting solidification microstructure at casting speed of 8 m/min: (a) Simulated results of roll casting structure; (b) Experimental results of roll casting structure

capacity of grain nucleus formed on roller surface free to liquid zone is enhanced, making the proportion of columnar grains decrease while equiaxed grains increase. When the casting speed increases to a certain value, in thin-gauge high-speed casting, columnar grains all convert into equiaxed grains in solidification microstructure. Fig.2(b) shows that simulated and experimental results agree well.

5 Conclusions

1) Nucleation and growth model based on CA was used to simulate the microstructure of twin-roll casting aluminum. The simulated and experimental results agree well, which provides a theoretical basis to find out the formation law in the process of roll casting solidification through numerical simulation.

2) Solidification microstructure is different as a result of different casting speed. When the casting speed is 1.3 m/min, under conditions of conventional roll casting, coarse columnar grains dominate the solidification microstructure, and equiaxed grains exist in the center of aluminum strip. When the casting speed continuously increases to 8 m/min, that is, under the

conditions of thin-gauge high-speed casting, columnar grains in solidification structure all convert into equiaxed grains.

References

- [1] WANG Y C, BECKRMANN C. Multi-scale/-phase modeling of dendritic alloy solidification [J]. ASME Heat Transfer Division, (Publication) HTD, Transport Phenomena in Solidification, 1994, 284: 75–95.
- [2] BROWN D J, HUNT J D. A model of columnar growth using a front-tracking technique [C]// Modeling of Casting, Welding and Advanced Solidification Processes XI. Aachen Germany, 2000: 437–444.
- [3] ZHAO H D, LIU B C. Modeling of stable and metastable eutectic transformation of spheroidal graphite iron casting [J]. ISIJ International, 2001, 41(9): 986–991.
- [4] DIEPERS H J, BECKRMANN C, STEINBACH I. Simulation of convection and ripening in a binary alloy much using the phase field method [J]. Acta Mater, 1999, 47(3): 3663–3678.
- [5] NESTLER B, WHEELER A A. Multi-phase-field method of eutectic and peritectic alloys: Numerical simulation of growth structures [J]. Physica D: Nonlinear Phenomena, 2000, 138(1): 114–133.
- [6] TONG X, BECKRMANN C, KARMA A, DIEPERS H J, STEINBACH I. Phase-field simulation of dendritic crystal growth in a forced flow [J]. Phy Rev E, 2001, 63(6): 1–16.
- [7] ZHANG G Y, JING T, LIU B C. Microstructure simulation of aluminum alloy casting using phase field method [J]. Int J Cast Metal Res, 2002, 15(13): 237–240.
- [8] ZHU Yao-chan, YANG Gen-cang, WANG Jin-cheng, ZHAO Da-wen, FAN Jian-feng. Multi-phase field simulation of uni-directional solidification for binary eutectic alloys [J]. The Chinese Journal Nonferrous Metals, 2005, 15(7): 1026–1032. (in Chinese)
- [9] LI Xin-zhong, GUO Jing-jie, SU Yan-qing, WU Shi-ping, FU Heng-zhi. Phase-field simulation of dendritic growth for binary alloys with complicate solution models [J]. Trans Nonferrous Met Soc China, 2005, 15(4): 769–776.
- [10] SPITTLE J A, BROWN S G R. Computer simulation of the effects of alloy variables on the grain structure of castings [J]. Acta Metall, 1989, 37(7): 1803–1810.
- [11] ZHU P, SMITH R W. Dynamic simulation of crystal growth by Monte Carlo method (I): Model description and kinetics [J]. Acta Metall Mater, 1992, 40(4): 683–692.
- [12] JIN Jun-ze, WANG Zhong-ting, ZHENG Xian-shu, YAO Shen. Study on the simulation of solidification structure [J]. Acta Metallurgica Sinica, 1998, 34(9): 928–932. (in Chinese)
- [13] RAPPAZ M, GANDIN C A. Probabilistic modeling of microstructure formation in solidification process [J]. Acta Metall Mater, 1993, 41(2): 346–360.
- [14] GANDIN C A, RAPPAZ M. Coupled finite element-cellular automation model for the prediction of dendritic grain structures in solidification process [J]. Acta Metall Mater, 1994, 42(7): 2233–2246.
- [15] ZHU M F, HONG C P. A modified cellular automation model for the simulation of dendritic growth in solidification of alloys [J]. ISIJ International, 2001, 41(5): 436–445.
- [16] XU Q Y, LIU B C. Modeling of as-cast microstructure of Al alloys with a modified cellular automation method [J]. Mater Trans Jim, 2001, 41(7): 2316–2321.
- [17] LI Q, BECKRMANN C. Scaling behavior of three dimensional dendrites [J]. Phy Rev E, 1998, 57(3): 3176–3188.
- [18] NASTAC L. Numerical modeling of solidification morphologies and segregation patterns in cast dendritic alloys [J]. Acta Metall Mater, 1999, 47(17): 4253–4262.
- [19] STEFANESCU D M, PANG H. Modeling of casting solidification, stochastic or deterministic [J]. Canadian Metallurgical Quarterly, 1998, 37(3/4): 229–239.
- [20] DILTHEY U, PAVLIK V. Numerical simulation of dendrite morphology and grain growth with modified cellular automata [C]// San Diego, USA: Modeling of Casting, Welding and Advanced Solidification Processes , 1998: 589–596.
- [21] XU Qing-yan, FENG Wei-ming, LIU Bai-cheng. Coupled macro-micro modeling for prediction of grain structure of Al alloy [J]. Trans Nonferrous Met Soc China, 2004, 14(1): 71–77.
- [22] KANG Xiu-hong, DU Qiang, LI Dian-zhong, LI Yi-yi. Modeling of the solidification by coupling Cellular Automaton with macro-transport model [J]. Acta Metallurgica Sinica, 2004, 40(5): 452–456. (in Chinese)
- [23] CHEN Jin, ZHU Ming-fang, SUN Guo-xiong. Numerical simulation on free dendrite growth in undercooled melt using using Cellular Automaton method [J]. Acta Metallurgica Sinica, 2005, 41(5): 799–803. (in Chinese)

(Edited by YANG Bing)